Fabrication of Anisotropic Regular Nanostructures on GaAs Surface due to Normal Incidence Ion Irradiation: A study on Temperature Dependence

Debasree Chowdhury and Debabrata Ghose

Saha Institute of Nuclear Physics, Sector-1, Block-AF, Bidhan Nagar, Kolkata 700064, India

Email: debasree.chowdhury@saha.ac.in

Abstract. We have carried out an investigation on nanostructure evolution of GaAs(100) surface due to normal incidence of threshold energy ion irradiation at different elevated temperatures. Well-ordered ripple nanopatterns are observed above 350°C near to surface recrystallization temperature where ripple wave-vector is oriented along $1\bar{1}0$ crystallographic direction on sample surface. The evolution of temperature induced ripple patterns at normal incidence can be attributed to the diffusion bias induced surface instability arising due to Ehlrich-Schwoebel (ES) barrier.

1. Introduction

In recent years, the fabrication of crystalline semiconductor nanostructures through self-organization or self-assembly processes seeks attention for unfolding the pattern evolution mechanism as well as for their several technological possibilities. Crystalline patterns on GaAs surface is of particular relevance for their unique optical and electrical properties and, for tremendous application in opto-electronics [1] and semiconductor device technology [2]. One of the possibilities to achieve crystalline nanostructures by self-organized process is molecular beam epitaxy (MBE) [3, 4, 5, 6] where the growth mechanism is governed by diffusion of deposited atoms restricted by surface crystallography at elevated temperatures. In case of homoepitaxy, when adatoms try to ascend the step edges, the diffusion of adatoms gets reflected by an additional barrier, known as Ehrlich-Schwoebel (ES) barrier, causes an uphill current and therefore results into mound or pyramid-like structures [7]. However, the epitaxial growth of nanostructures requires ultrahigh vacuum conditions and is also somewhat complex and cost-intensive. On the other hand, ion irradiation is a simple, inexpensive technique to fabricate surface patterns in nanoscale over large area (~ mm^2) within short time (~min) on various kind of solids, e.g. semiconductors, insulators and metals [8]. By controlling different processing parameters like ion incidence angle, ion sputtering time, substrate rotation etc., there are enormous possibilities of fabricating different kind of nanostructures like ripples, dots, checker-board patterns, conical structures of predictable size and shape just in one step. There is no need of masking and there are no chemical hazards.

Among various structures, the anisotropic patterns like ripples are generally observed due to oblique incidences ion irradiation at room temperature. These ripples usually lies either perpendicular or parallel to ion beam projection and are observed in angular region of 55-70° and 80-85° respectively. The evolution of ripples at room temperature due to oblique incidence ion irradiation can be explained by BH model [9] where surface instability during ion irradiation is thought to be a competitive interplay between curvature dependent ion erosion and surface smoothening via. surface diffusion. Ripple structure at normal incidence was first reported by Valvusa et. al. on Ag (110) surface in a restricted temperature range 270-320 K [10]. The evolution of ripples at normal incidence on metal (Ag) surface was attributed to an additional instability arising due to presence of ES barrier associated with the crystal type, symmetry and orientation [11]. Metal surfaces remain crystalline even after ion irradiation at room temperature. Whereas, the semiconductor surfaces undergoes into an amorphization of upper surface during irradiation at room temperature on which ES barrier does not exist. Thus, the amorphized layer diminishes the probability of obtaining anisotropic structures on semiconductor surface at room temperature due to normal incidence ion irradiation as well as it reduces the quality factor of nanostructures in application perspective. The last one is a major drawback against huge possibilities of IBS technique. The crystalline structure, however, can be retrieved by performing ion sputtering on substrates at or above its re-crystallization temperature.

Recently, we have reported the temporal evolution of crystalline nanoripples on GaAs(100) surface sputtered by threshold energy ions at normal incidence above the re-crystallization temperature [12]. The ridges of the ripples are found to align along the $1\bar{1}0$ direction and follow the twofold symmetry of the bombarded crystal surface. These patterns are quite resembled with the elongated mound structures developed in case of homoepitaxial growth of GaAs but the ordering is not such regular there [3, 4]. Similar kind of ripple patterns but with high degree of regularity on GaAs(100) surface were reported by Ou et al. [13] where bombardment was performed by 1 keV Ar^+ ions at normal incidence and at elevated temperature 410°C. The evolutions of highly regular ripples were explained by self-assembly of ion induced vacancies driven by ES barrier [13]. For irradiation with high ion energy (1 keV), the probability of surface vacancy production is quite high rather than the surface adatoms. This is because the energy, which transfers from high-energy ions to substrate atoms during bombardment, is sufficiently high enough that, even after suffering from a series of collisions, they can easily overcome the surface binding energy and get sputtered away by leaving a corresponding vacancy there. Here, we report the temperature evolution of nanoripples on GaAs(100) surfaces from 20-450°C due to near-threshold energy (30 eV) ion sputtering. For threshold energy ions, as it is near to lattice displacement energy ~ 15 eV, sputtering yield is minimum. In this case, the energy of most of the primary knock-on atoms is significantly low and do not possessed enough kinetic energy to leave the surface after overcoming their surface binding energy. Thus, the population of surface defects produced by threshold energy ions in form of adatoms are comparable or higher than the vacancies. This study helps to understand the temperature induced pattern evolution mechanism mediated by surface diffusion of both adatoms and vacancies instead of sputter erosion which is considered as dominant cause of arising surface instability during sputtering [9].

2. Experimental Procedure

Ion irradiation was performed on commercially available GaAs (001) wafers by 30 eV Ar^+ ions at normal incidence and at different elevated temperatures from 20°C to 450°C for ion fluence 1×10^{19} cm^{-2}. Before sputtering, the substrates were ultrasonically cleaned by acetone to remove the organic contaminations. The experiments were performed in a broad beam high current ion beam system (M/s Roth & Rau Microsystems GmbH, Germany) where an inductively coupled RF discharge ion source was employed to extract ion beam of diameter approximately 4 cm by using three graphite grid ion optical system [12]. The substrate temperature was raised using a radiation heater from the front side. During irradiation, the current density was fixed around 40 $\mu A.cm^{-2}$ and the chamber pressure was of the order of 10^{-4} mbar. The sputtered samples were characterized by Atomic Force Microscopy (AFM) operating in tapping mode with a nominal tip radius of 10 nm using a Nanoscope IV multimode SPM.

3. Experimental Results & Discussions

Figure 1 shows AFM images of GaAs(100) surfaces irradiated by 30 eV Ar^+ ions at normal incidence and at different substrate temperatures (T) for ion fluence $\varphi \sim 1\times 10^{19}$ cm^{-2}. The surfaces remain flat below 350°C. A faint or poorly ordered ripple structures are found to appear on surface at T=350°C.

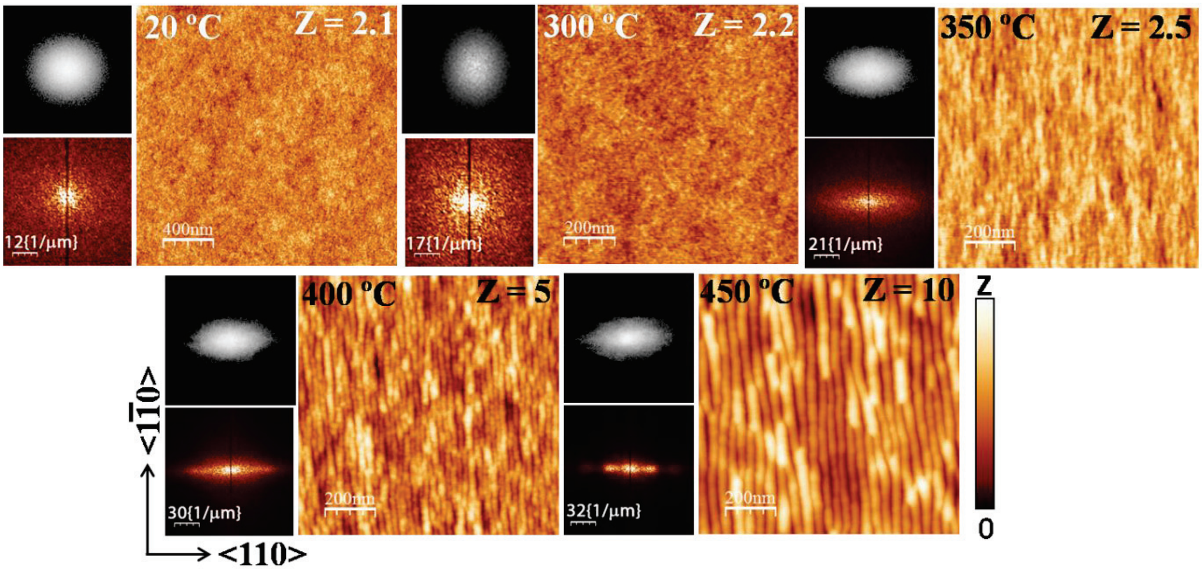

Figure 1. The AFM images of 30 eV Ar^+ ion irradiated GaAs (001) surfaces at fluence 1×10^{19} cm^{-2} for different substrate temperatures. Z denotes vertical length scale in nm. The corresponding FFT and 2-D angle distributions are shown beside the left side of AFM images. All the ion irradiation experiments were performed at 0° with respect to surface normal.

The wave-vector of theses ripples are aligned along <110> crystallographic direction of GaAs(001) surface. With increase of T, the ripples become longer and more regular. This can be confirmed by the corresponding FFT images. The circular spot corresponds to 20°C is begin to elongate along <110> direction with subsequent increase of T and at 450°C, the appearance of higher order diffraction spots on either side of the central bright spot reveals the increase in ripple ordering. Furthermore, the two-dimensional angle distributions corresponding to the AFM images for T ≥ 300°C shows two-fold symmetry along <110> direction, indicate the formation of well-defined facets along that specified direction.

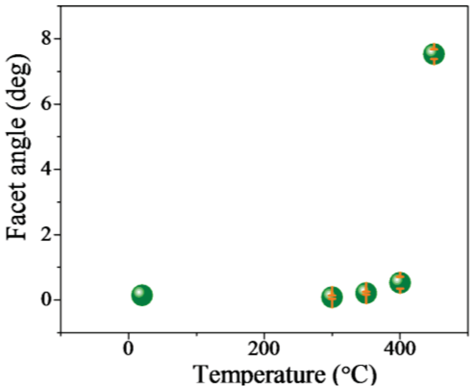

Figure 2. The facet slope m as a function of substrate temperature T.

The facet angles i.e., the local slope $m = \vec{\nabla} h$ of faceted structures with respect to substrate surface can be estimated from one dimensional angle distribution along ⟨110⟩ direction and its variation with temperature is shown in figure 2. Around 450°C, the slope value reaches a maximum of 7.5°. This identifies the development of the facet plane {108} (7.1°) with respect to the (001) surface. Such a slope selection, in the continuum description of kinetic instabilities, is associated with the surface diffusion mediated by Ehrlich-Schwoebel (ES) barrier and is encoded with zero diffusion current [14].

For detail characterization of the temperature induced surface morphologies, height-height correlation functions $G(l,t) \sim \langle [h(l,t) - h(0,t)]^2 \rangle$ have been extracted from the AFM images along its fast scan axis (x-direction), i.e., along $\langle 110 \rangle$ crystallographic direction and is represented by figure 3(a). For the scale invariant and isotropic surface, $G(l,t)$ shows the following properties:

$$G(l,t) = \begin{cases} l^{2\alpha} & \text{for } l \ll \xi \\ W^2(t) & \text{for } l \ll \xi \end{cases} \quad (1)$$

where, α, W and ξ are the roughness exponent, rms roughness and the lateral correlation length respectively. The values W and α are calculated from equation 1 and their variation with temperature is shown by figure 3(b) and 3(c) respectively. Around T ~ 325-350°C, the rms roughness (W) of irradiated surface increases slightly due to appearance of faint ripple topographies and beyond 350°C, it shows a steep rise with T. On the other hand, α also shows an increase beyond 300°C and exhibits a value around 0.7 at highest T ~ 450°C. This α value is again close to the theoretically estimated value for the ES barrier dominated kinetic instabilities [15].

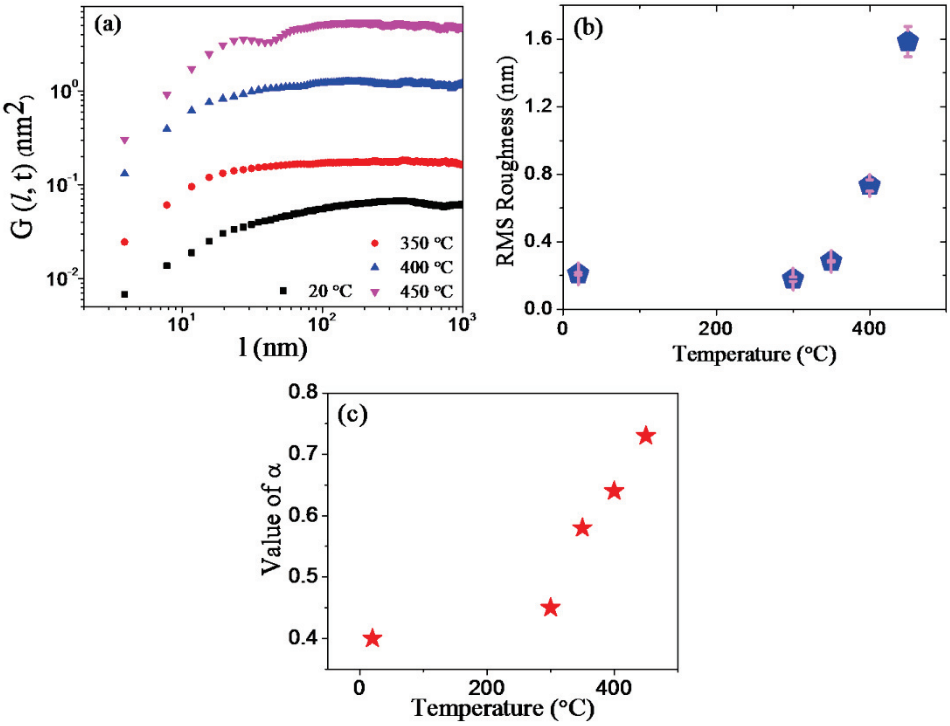

Figure 3. (a) Logarithmic plot of Height-height correlation function (HHCF) vs. lateral distance l, corresponds to different temperatures; (b) Plot of the surface roughness W and (c) roughness exponent α with substrate temperatures.

The correlation length ξ is basically the extent up to which the lateral correlation of the system exists and defines by the width of the auto-correlation function $C(l) = \langle h(l)h(0) \rangle$ at which $C(\xi) = C(0)/e$, e being the base of natural logarithm [16] $C(l)$ corresponds to different temperatures are extracted from the corresponding AFM images and are shown by figure 4. The correlation lengths ξ for different temperatures are calculated from the corresponding curves displayed in figure 4(a) and are represented by figure 4(b) which again shows an increase of correlation length after substrate temperature 300°C.

The above described results imply that the high substrate temperature strongly influences the growth of ripple nanopatterns on GaAs surfaces. When the temperature is much lower than the surface recrystallization temperature T_R (~300°C for GaAs(100) surface [17]), the surface remains in amorphous state and no atomic steps are available. In this case, the observed surface smoothening below T_R is dominated by the transport of defects between regions of negative surface curvature and positive curvature [18]. induced bulk defects and disorders are dynamically annealed and the surface

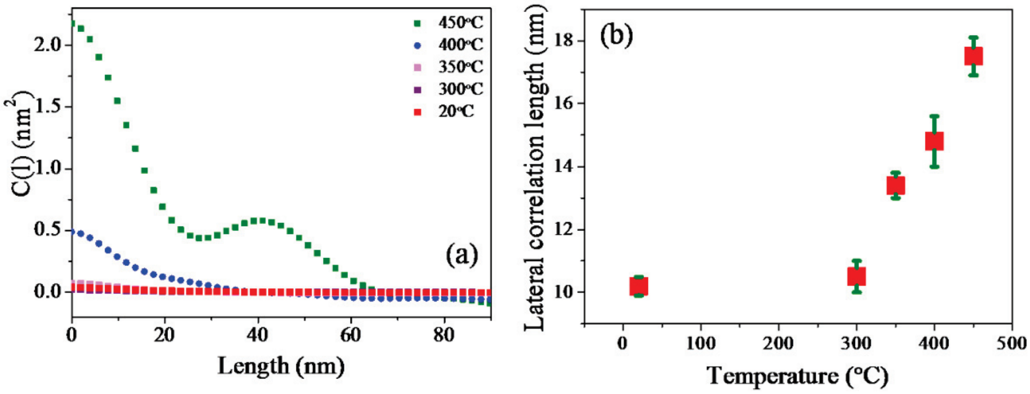

Figure 4. (a) Auto-correlation function $C(l)$ vs. lateral distance l for different temperatures; (b) The plot of lateral correlation length ξ vs. temperature.

become crystalline comparable with that of virgin GaAs surface. For the case of crystalline surface, the patterns formation is governed by the surface diffusion of adatoms and vacancies hindered by the presence of ES barrier, exists on terraces, terrace steps and kinks. Here, it is to be mentioned that as threshold energy ions of energy 30 eV is close to the lattice displacement energy ~ 20 eV, the sputtering is suppressed but, simultaneously, it drives the production of a large number of defects on surfaces in form of adatoms, vacancies and their higher ordered clusters. On a stepped surface of small slope (m), whenever adatoms try to descend a step edge or the vacancies tend to climb up to a higher terrace, they gets reflected by ES barrier and will generate uphill or downhill current of the diffusing species [19]. This nonzero diffusion currents cause an unbound growth of surface slope. In actual case, the uphill current (if adatoms are the dominant diffusion species) is counterbalanced by "downhill funnelling" current [20] which results into stable patterns with well-defined facets by surface reorganization. Further increase of substrate temperature, above T_R i.e., 450°C leads the surface towards more crystallinity and makes the effect of ES barrier more strong. This generates more reflection of adatoms (or vacancies), and thus, enhances the diffusion current which is responsible for high rise of facets as well as more regular ripple patterns at this temperature. In ref. [12], we examine the micro-structure of ion irradiated GaAs surface at temperature 450°C by high-resolution transmission electron microscopy (HRTEM) which confirms the crystallinity of the sample surface.

For ES barrier driven surface-diffusion processes, the evolution of surface height during ion sputtering can be expressed by:

$$\frac{\partial h}{\partial t} + \nabla . j = 0 \qquad (2)$$

where j is the total surface current due to diffusion and is classified into two components: (i) the classical Herring–Mullins (HM) diffusion current [21] $j_{HM} \sim \nabla(\nabla^2 \mathrm{h})$; and (ii) the non-equilibrium slope-dependent current $j_{ES} \sim m_{x,y}\left(1 - \delta m_{x,y}^2\right)$ due to ES instabilities, where the first and second term corresponds to the destabilized uphill current and downward current respectively [15, 19, 22]. x and y corresponds to the crystallographic directions $\langle 110 \rangle$ and $\langle 1\bar{1}0 \rangle$ respectively. The uphill currents along these two directions, $j_{\langle 110 \rangle}$ and $j_{\langle 1\bar{1}0 \rangle}$ are not equivalent in terms of ES barrier heights and activation energies of surface diffusion [23, 24]. Again, Ga atoms, on GaAs(001) surface, possesses ES barrier only along $\langle 110 \rangle$ but not along $\langle 1\bar{1}0 \rangle$ [23]. On the other hand, no ES barrier exists for As adatoms [23]. Thus, intra-layer diffusion of Ga is possible along $\langle 1\bar{1}0 \rangle$, but the interlayer diffusion along $\langle 110 \rangle$ is blocked by ES barrier which results in a destabilizing uphill current running perpendicular to $\langle 110 \rangle$. This is responsible for evolution of ripples with wave vector along $\langle 110 \rangle$ direction. δ in j_{ES} is related to the facet angle θ by the relation $\tan\theta = \pm 1/\delta$ where the net uphill and downhill ES current becomes zero. In our case $\theta \sim 8°$, which sets δ=50. The numerical integration of Equation 2 with $\delta \sim 50$ can well predict the formation of ripple nanostructures comparable with the experimental results and are illustrated briefly in our recent work [12].

4. Conclusion

In summary, we have studied the temperature induced dynamics of nanostructures on GaAs(100) surface due to normal incidence near-threshold energy (30 eV) Ar^+ ion beam sputtering. Anisotropic nanoripple patterns are evolved when the substrate is elevated near or above the surface recrystallization temperature. Ripple amplitude, ordering and lateral correlation length is found to improved with increase of substrate temperature. The ripple alignment follows the crystal symmetry of the bombarded surface. This phenomenon is attributed to the anisotropic diffusion of the adspecies (adatoms, vacancies) hindered by the Ehrlich-Schwoebel barrier.

5. Acknowledgement

One of the authors, (DG) as Emeritus Scientist, CSIR, want to acknowledge CSIR (Grant No. 21(0988)/13/EMR-II dated 30-04-2015), New Delhi for financial support.

References

[1] Dimakis E, Jahn U, Ramsteiner M, Tahraoui A, Grandal J and Kong X 2014 *Nano. Lett.* **14** 2604-09
[2] Baca A G and Ashby C I H 2009 Fabrication of GaAs devices (IET) 6
[3] Apostolopoulos G, Herfort J, Däweritz L, Ploog K H and Luysberg M 2000 *Phys. Rev. Lett.* **84** 3358 (2000)
[4] Ballestad A, Ruck B J, Schmid J H, Adamcyk M, Nodwell E, Nicoll C and Tiedje T 2002 *Phys. Rev. B* **65** 205302
[5] Vidal F, Etgens V H, Fernandes V, Rache Salles B and Eddrief M 2011 *Phys. Rev. B* **83** 121305 (R)
[6] Mongeot F B D, Costantini G and Boragno C 2000 Phys. Rev. Lett. **84** 2445
[7] Mongeot F B D, Costantini G and Boragno C 2005 Appl. Phys. Lett. **87** 181916
[8] Muñoz-García J, Vázquez L, Cuerno R, Sánchez-García J A, Castro M, Gago R 2009 *Toward functional nanomaterials* ed Z M Wang (Dordrecht: Springer) pp 323–398
[9] Bradley R M and Harper J M E 1988 *J. Vac. Sci. Technol. A* **6** 2390
[10] Rusponi S, Boragno C and Valbusa U 1997 *Phys. Rev. Lett.* **78** 2795
[11] Valbusa U, Boragno C and Mongeot F B D 2002 *J. Phys.: Cond. Mat.* **14** 8153
[12] Chowdhury D, Ghose D, Mollick S A, Satpati B and Bhattacharyya S R 2015 *Phys. Stat. Sol. B* **252** 811-15
[13] Ou X, Heinig K -H, Hübner R, Grenzer J, Wang X, Helm M, Fassbender J and Facsko S 2015 *Nanoscale* **7** 18928-35
[14] Levandovsky A and Golubović L 2015 *Phys. Rev. E* **7** 18928
[15] Siegert M and Plischke M 1994 *Phys. Rev. Lett.* **73** 1517
[16] Zhao Y –P, Drotar J T, Wang G C and Lu T M 1999 *Phys. Rev. Lett.* **82** 4882
[17] Mazey D J and Nelson R S 1969 *Radiat. Eff.* **1** 229-239
[18] Moseler M, Gumbsch P, Casiraghi C, Ferrari A C, Robertson J 2005 *Science* 2005 **309** 1545-48
[19] Barabási A L and Stanley H E 1995 Fractal concepts in surface growth (New York, Australia: Cambridge university press)
[20] Michely T and Krug J 2012 Islands, mounds and atoms vol 42 ed Ertl G, Lüth H and Mills D L (New York: Springer Science & Business Media)
[21] Mullins W W 1959 *J. Appl. Phys.* **30** 77-83
[22] Siegert M 1998 *Phys. Rev. Lett. 81* 5481
[23] Salmi M A, Alatalo M, Ala-Nissila T and Nieminen R. M. 1999 *Surf. Sci.* **425**, 31-47
[24] Shitara T, Vvedensky D D, Wilby M R, Zhang J, Neave J. H. and B. A. Joyce 1992 *Phys. Rev. B* **46**, 6825.